Steady-State and Dynamic Properties of Cardiac Sodium-Calcium Exchange

Secondary Modulation by Cytoplasmic Calcium and ATP

DONALD W. HILGEMANN, ANTHONY COLLINS, and SATOSHI MATSUOKA

From the Department of Physiology, University of Texas Southwestern Medical Center at Dallas, Dallas, Texas 75235

ABSTRACT Dynamic responses of cardiac sodium-calcium exchange current to changes of cytoplasmic calcium and MgATP were monitored and analyzed in giant membrane patches excised from guinea pig myocytes. Secondary dependencies of exchange current on cytoplasmic calcium are accounted for in terms of two mechanisms: (*a*) The sodium-dependent inactivation process, termed I_1 modulation, is itself strongly modulated by cytoplasmic calcium. Recovery from the I_1 inactivated state is accelerated by increasing cytoplasmic calcium, and the calculated rate of entrance into I_1 inactivation is slowed. (*b*) A second modulation process, termed I_2 modulation, is not sodium dependent. As with I_1 modulation, the entrance into I_2 inactivation takes place over seconds in the absence of cytoplasmic calcium. The recovery from I_2 inactivation is a calcium-dependent transition and is rapid (<200 ms) in the presence of micromolar free calcium. I_1 and I_2 modulation can be treated as linear, independent processes to account for most exchange modulation patterns observed: (*a*) When cytoplasmic calcium is increased or decreased in the presence of high cytoplasmic sodium, outward exchange current turns on or off, respectively, on a time scale of multiple seconds. (*b*) When sodium is applied in the absence of cytoplasmic calcium, no outward current is activated. However, the full outward current is activated within solution switch time when cytoplasmic calcium is applied together with sodium. (*c*) The calcium dependence of peak outward current attained upon application of cytoplasmic sodium is shifted by ~ 1 log unit to lower concentrations from the calcium dependence of steady-state exchange current. (*d*) The time course of outward current decay upon decreasing cytoplasmic calcium becomes more rapid as calcium is reduced into the submicromolar range. (*e*) Under nearly all conditions, the time courses of current decay during application of cytoplasmic sodium and/or removal of cytoplasmic calcium are well fit by single exponentials. Both of the modulation processes are evidently affected by MgATP.

Address reprint requests to Donald W. Hilgemann, Department of Physiology, University of Texas Southwestern Medical Center at Dallas, 5323 Harry Hines Boulevard, Dallas, TX 75235.

J. GEN. PHYSIOL. © The Rockefeller University Press · 0022-1295/92/12/0933/29 $2.00
Volume 100 December 1992 933–961

Similar to the effects of cytoplasmic calcium, MgATP slows the entrance into I_1 inactivation and accelerates the recovery from inactivation. MgATP additionally slows the decay of outward exchange current upon removal of cytoplasmic calcium by 2–10-fold, indicative of an effect on I_2 inactivation. Finally, the effects of cytoplasmic calcium on sodium-calcium exchange current are reconstructed in simulations of the I_1 and I_2 modulation processes as independent reactions.

INTRODUCTION

Cardiac sodium-calcium exchange function is strongly modulated by secondary reactions that are themselves dependent on cytoplasmic sodium and calcium concentrations (Hilgemann, 1990*a*). A sodium-dependent inactivation process takes place on a multisecond time scale, apparently from a fully sodium-loaded state, and can be explained as an intrinsic "gating" reaction from a fully active to an inactive state (Hilgemann, Matsuoka, Nagel, and Collins, 1992). The secondary modulation of sodium-calcium exchange by cytoplasmic calcium (DiPolo, 1979; Kimura, Miyamae, and Noma, 1987; Noda, Shepherd, and Gadsby, 1988; Rasgado-Flores, Santiago, and Blaustein, 1988; Miura and Kimura, 1989; for review of work in squid axon, see DiPolo and Beaugé, 1991) may also take place on a multi-second time scale (Hilgemann, 1990*a*). Interestingly, the stimulation of sodium-calcium exchange activity by MgATP (DiPolo, 1976, 1979; Blaustein, 1977; Rasgado-Flores et al., 1988; Hilgemann, 1990*a*) involves an apparent increase of affinity for cytoplasmic calcium in activating the calcium influx exchange mode (DiPolo and Beaugé, 1987; Collins, Somlyo, and Hilgemann, 1992) and a decrease in the ability of cytoplasmic sodium to inhibit calcium extrusion in squid axon (DiPolo, 1974; Requena, 1978). In cardiac giant membrane patches, the secondary actions of both cytoplasmic calcium and MgATP on the exchanger are coupled, at least in part, to the sodium-dependent inactivation process (Hilgemann, Collins, Cash, and Nagel, 1991). Both cytoplasmic calcium (Hilgemann, 1990*a*) and MgATP (Collins et al., 1992) diminish the extent of sodium-dependent inactivation. Given these interrelationships, it appeared important to examine in more detail how the secondary mechanisms may be linked to one another and to the exchange cycle itself. In this article, the interactions of cytoplasmic calcium and sodium in the secondary modulation of sodium-calcium exchange are presented and analyzed. Most of our observations on the secondary exchange kinetics appear consistent with the existence of two modulation reactions. Under some conditions, the existence of additional inactive and active exchanger states appears probable. In the Appendix, simple simulations are presented that show how two parallel inactivation processes may account for many of the exchanger gating properties.

METHODS

The experimental methods and solutions used in this study were the same as described in the previous article (Hilgemann et al., 1992). All results presented are from giant patches taken from guinea pig ventricular cells.

RESULTS

Cytoplasmic Calcium and Sodium Do Not Compete at a Secondary Activation Site

As described in the Introduction, cytoplasmic sodium and calcium interact antagonistically in the secondary modulation of sodium-calcium exchange. As shown in Fig. 1, the secondary calcium dependence of outward exchange current indeed depends on the degree of activation by cytoplasmic sodium. Fig. 1 shows the cytoplasmic calcium dependence of steady-state outward current at 90 and at 18 mM cytoplasmic sodium. The extracellular calcium concentration is 5 mM. Half-maximum free cytoplasmic calcium concentrations are 1.8 and 0.8 μM, respectively. Hill slope coefficients are 1.40 and 1.46, respectively. While these results are indicative of an antagonistic interaction, they probably do not reflect direct competition between sodium and calcium at a regulatory site. First, the calcium dependence is shifted here by a factor

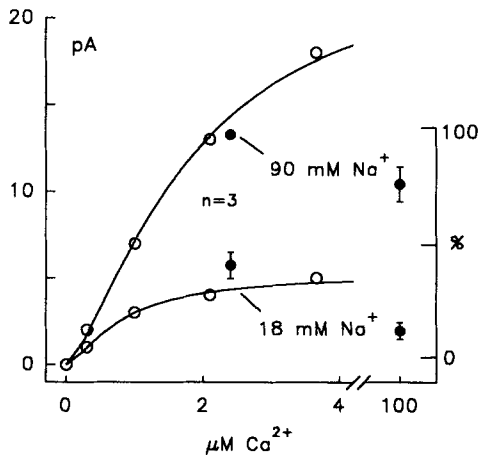

FIGURE 1. Cytoplasmic calcium dependence of the steady-state outward current. Extracellular calcium concentration is 5 mM. The steady-state outward currents activated by 90 and 18 mM in the same patch are plotted against cytoplasmic calcium concentration (*open circles*). Solid lines are fitted with a Hill equation; half-maximum calcium concentrations are 1.8 and 0.8 μM, respectively, and the Hill coefficients are 1.40 and 1.46, respectively. Filled circles show steady-state current amplitudes at 2.5 and 100 μM calcium in other patches. The data are normalized to the amplitude at 2.5 μM calcium and 90 mM sodium and presented as means ± SE (n = 3).

of only 2.2 for a fivefold change of cytoplasmic sodium. Second, the concentration–current relation for cytoplasmic sodium in activating the outward exchange current is monotonic (e.g., Hilgemann, 1990*a*). If sodium and calcium competed directly at the regulatory site(s), high sodium would displace calcium from regulatory sites with the result of a bell-shaped concentration–current relation. This has not been observed (>20 observations).

Filled circles represent another set of experiments in which the effect of a higher calcium concentration (100 μM) was studied. Steady-state currents were measured at 2.5 and 100 μM cytoplasmic calcium in the presence of 18 and 90 mM cytoplasmic sodium and normalized to the current amplitude at 90 mM sodium and 2.5 μM calcium (n = 3). At 100 μM calcium the current decreased by 22% at 90 mM sodium and by 78% at 18 mM sodium. The inhibition of the outward current by cytoplasmic calcium is due to the competitive action of calcium at the transport site, and this

mechanism is further studied in an accompanying article (Matsuoka and Hilgemann, 1992).

Experimental Definition of Two Modulation Processes

Fig. 2 presents the characteristic pattern of current transients obtained routinely when outward exchange current is activated by rapid application of cytoplasmic

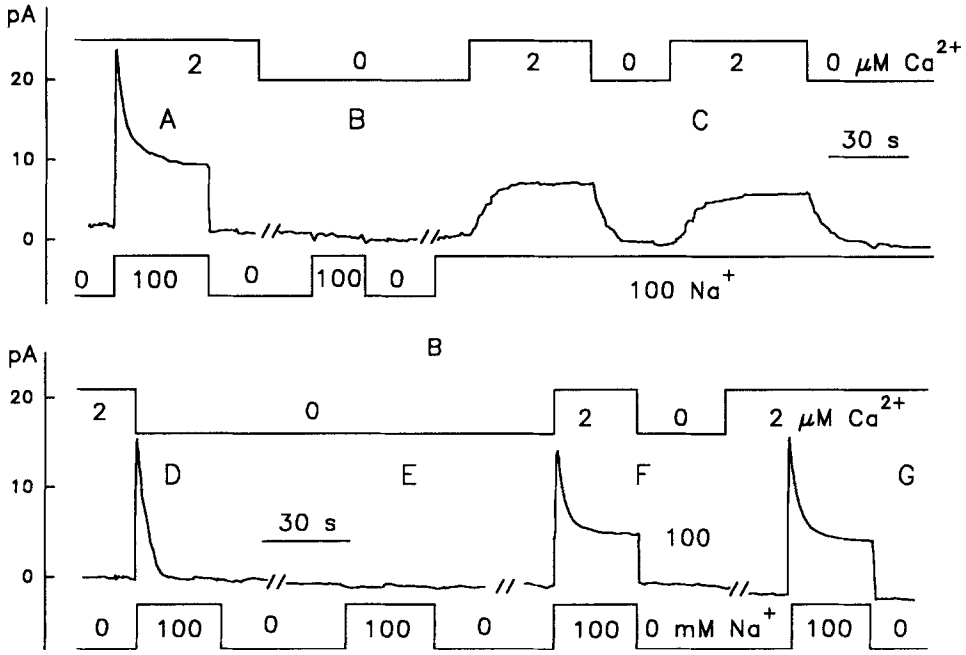

FIGURE 2. Rapid and slow calcium-dependent recovery of outward exchange current from inactivation. Pipette solution A (with no sodium and 5 mM calcium). Outward exchange current activated with 100 mM cytoplasmic sodium as indicated below records, and with and without 2 μM cytoplasmic free calcium as indicated above records. (*Top*) Exchange current was first activated entirely in the presence of 2 μM free calcium (*A*). Next, calcium-free solution was applied. No current was activated by 100 mM sodium in the absence of calcium (*B*). In the final portion of the upper panel, 2 μM free calcium-containing solution was superfused twice in the presence of sodium (*C*). Note that the slow turn-on and turn-off of the outward current in the presence of sodium takes many seconds. (*Bottom*) Continuing from the upper panel, a solution switch was made from calcium-containing, sodium-free solution to one without calcium but with sodium (*D*). Note that peak current is of equal magnitude to the control transient, but the current decays over seconds to zero. Next, activation was again attempted entirely in calcium-free solution (*E*). Thereafter, sodium and calcium were applied together upon switching from a calcium-free, sodium-free solution (*F*). Peak current was almost as large as the control transient with some rounding of the peak. Finally, in the lower panel a control current transient was again performed to check current run-down (*G*).

sodium and/or calcium (>20 observations). The records are presented in the sequence of the experiment. Breaks in the records mark time periods where solution lines were cleared of a solution and/or an observation was repeated. The result marked *A* is the usual outward exchange current transient obtained upon applying

100 mM sodium in the presence of 2 μM cytoplasmic free calcium. The current decays over 15 s by ~50% and reaches steady state at ~40% of the peak value obtained. As shown in record *B*, no exchange current could be activated by applying sodium in the absence of calcium. When 2 μM free calcium is applied in the presence of 100 mM sodium (records in C), the outward exchange current turns on over the course of 15 s and turns off similarly slowly when calcium is removed.

For the records in part *D*, solutions were switched between one with 2 μM free calcium and no sodium to one with sodium but without calcium. The peak current obtained is 20% smaller than that obtained in *A*, but only a few percent smaller than the final control transient in *G*. The current decays to essentially zero within 10 s. In part *E* of the records, sodium was again applied in the absence of calcium and no current could be activated. In part *F*, by contrast, calcium was applied together with sodium in a switch from the zero sodium, zero calcium solution. In this case, an outward current is activated that is nearly the magnitude of peak current activated subsequently in part *G* with the usual switch to sodium in the continued presence of calcium. Since no current can be activated upon applying sodium in the absence of calcium, the exchanger must be in an inactive state in the absence of calcium. Since nearly full current can be activated immediately by application of calcium together with sodium, the recovery from that inactive state must take place in the same (or a shorter) time frame as the solutions switches accomplished here (~200 ms).

From the >20 experiments the following observations appear noteworthy. The fast activation of outward exchange current upon application of calcium and sodium, as in *F*, was sometimes clearly slower than the solution switch time (i.e., >200 ms), and the peak current obtained upon applying cytoplasmic calcium with sodium was then substantially less than peak current obtained upon applying sodium after preapplying calcium (as in *A*, *D*, and *G*). In some cases, the outward current reached values only slightly greater than the steady-state current. In such myocyte batches, a similar time dependence in the activation of the *inward* exchange current by cytoplasmic calcium could also be resolved (results not presented).

It seems impossible to explain these behaviors without assuming the existence of two types of modulatory reactions, and subsequent protocols were planned on this basis. For clarity in presenting the rationales of experiments, the two hypothetical modulation processes will be termed I_1 and I_2 modulation. I_1 will refer to the sodium-dependent inactivation process (i.e., related to the decay of current upon application of sodium) and I_2 modulation will refer to the sodium-independent process that moves the exchanger to an inactive state in the absence of cytoplasmic calcium. The term calcium-dependent activation is not used in this article because both modulation processes are evidently affected by cytoplasmic calcium. The designations used are consistent with the I_1 and I_2 inactive states used previously in an overview article (Hilgemann et al., 1991).

In the Appendix to this article, the two reactions are treated as independent processes,

$$1)\ A_1 \underset{\beta_1}{\overset{\alpha_1}{\rightleftarrows}} I_1 \qquad 2)\ A_2 \underset{\beta_2}{\overset{\alpha_2}{\rightleftarrows}} I_2$$

where A_1 and A_2 are the fractions of total exchanger population that have not

undergone the respective inactivation reactions. For clarity in the description of some results, reference will be made to the rate constants in this diagram, where α and β refer to the inactivation and recovery rate constants, respectively, of the two modulation reactions.

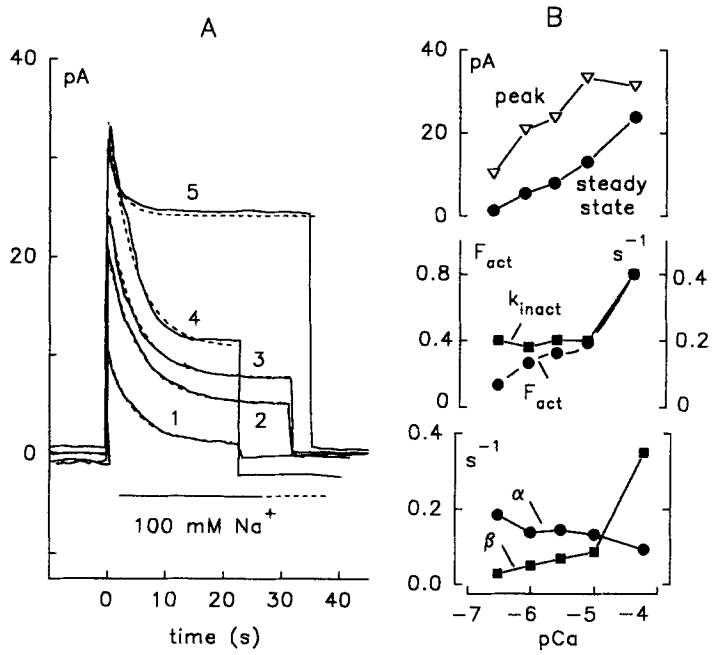

FIGURE 3. Outward exchange current transients obtained during application of 100 mM cytoplasmic sodium at different cytoplasmic calcium concentrations. (*A*) The results, numbered *1–5*, are with 0.3, 1, 3, 10, and 60 μM free calcium, respectively. Dotted curves in *A* are single exponentials, fitted to the experimental results by the least-squares method. Rate constants for results *1–5* are 0.21, 0.19, 0.21, 0.21, and 0.43 s^{-1}, respectively. (*B*) The peak (*open triangles*) and steady-state (*filled circles*) exchange current magnitudes are plotted in the upper graph. Note that the calcium dependence of peak exchange current shifts by ~1 log unit from the calcium dependence of steady-state exchange current. The rate constants (k_{inact}) and the ratio of steady-state current to peak current (F_{act}) are plotted in the middle graph. Calculated rate constants for inactivation (α) and recovery from inactivation (β) are plotted in the lower graph. See text for explanations.

Modulation of Sodium-dependent Inactivation by Cytoplasmic Calcium

As outlined up to now, sodium-dependent inactivation (I_1 inactivation) is in some way inhibited or reduced as cytoplasmic calcium is increased. Fig. 3 presents the usual effects of cytoplasmic calcium with kinetic analysis of the outward exchange current transients at different free calcium concentrations. Fig. 3 *A* shows current transients obtained in random order upon applying 100 mM cytoplasmic sodium in the presence of 0.3, 1, 3, 10, and 60 μM free cytoplasmic calcium, labeled 1–5,

respectively. An exponential function has been fitted to each of the transients and is plotted as a dotted line.

In Fig. 3 *B*, the results are plotted against the pCa of cytoplasmic solutions. The upper graph gives the peak (triangles) and steady-state current magnitudes (circles). As described previously (Hilgemann, 1990*a*), the calcium dependence of peak current is shifted to lower concentrations by ~1 log unit from the calcium dependence of steady-state current. Thus, as calcium is increased the difference between peak and steady-state current first increases and then decreases. Since the calcium dependence of the peak currents should not be influenced by the sodium-dependent (I_1) inactivation, this relationship may be assumed to reflect the steady-state function of I_2 modulation. The half-maximum free calcium concentration is routinely in the range of 0.3–0.6 μM.

In the middle graph, the rate constants of the current decays (k_{inact}) are plotted together with the ratio of steady-state current to peak current for each transient (F_{act}). Note that with free calcium concentrations up to 10 μM the rate constant is essentially constant at 0.2 s^{-1}. At 60 μM free calcium in this experiment, the rate constant is approximately doubled. In some experiments this acceleration was not observed, and it is noted that even with deregulation by chymotrypsin a small remaining decay component is sometimes observed. The ratio of steady-state current to peak current (F_{act}) increases from ~0.1 at 0.3 μM free calcium to ~0.4 at 10 μM free calcium and then up to 0.8 at 60 μM free calcium.

Hypothetical rate constants for the forward (α) and backward (β) reactions in the modulation process can be calculated, assuming a simple monomolecular process and that F_{act} and k_{inact} are determined exclusively by these reactions. Accordingly,

$$F_{act} = \beta/(\alpha + \beta)$$

and

$$k_{inact} = \alpha + \beta$$

Calculated rate constants are given in the bottom graph of Fig. 3 *B*. Up to 10 μM cytoplasmic free calcium, the hypothetical forward and reverse reactions roughly equally decrease and increase, respectively. At 60 μM free calcium the backward reaction is (hypothetically) greatly increased in rate. The prediction that both rate constants should change in response to a change of cytoplasmic calcium is consistent with an idea that calcium binding at a regulatory site stabilizes an active conformation of the exchanger, thereby both slowing the inactivation reaction and accelerating the recovery from inactivation.

Calcium Accelerates Recovery from I_1 Inactivation

While it is not possible to isolate the inactivation reaction from the recovery reaction, it is possible with appropriate protocols to isolate the recovery reaction. For the outward current, this is described in Fig. 4. To do so, sodium is applied in the presence of 1 μM free calcium until steady state is reached. The cytoplasmic solution is then switched for a variable period of time to one with a different chosen free calcium concentration and zero sodium (see representative current records in Fig. 4 *A*). The peak current magnitudes achieved upon reapplication of sodium with 1

μM free calcium should reflect the recovery from sodium-dependent inactivation. As described in Fig. 2, the I_2 process generally reaches steady state within solution switch times upon reapplying calcium. For this reason, the protocol just described can be carried out to follow recovery from sodium-dependent inactivation (I_1 inactivation) in the absence of cytoplasmic free calcium.

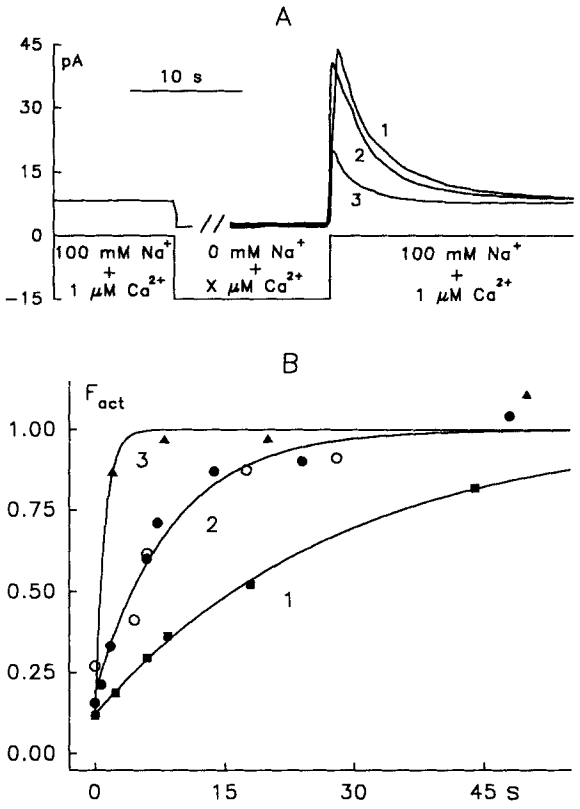

FIGURE 4. Recovery of outward exchange current from sodium-dependent inactivation. (*A*) The protocol used to determine time courses of recovery of outward exchange current from inactivation. As indicated, 100 mM sodium was applied with 1 μM free calcium until a steady state was achieved. Then the cytoplasmic solution was switched to a sodium-free solution with a variable free calcium concentration for a variable time period, and thereafter the original solution was reapplied. The result marked *1* is after a 48-s period in 2 μM free calcium, the result marked *2* is after calcium-free exposure for 45 s, and the result marked *3* is after calcium-free exposure for 13 s. (*B*) The peak current achieved upon reactivating the current is plotted against the time of sodium-free superfusion. The results are from two experiments. Open and filled circles give the results obtained in the two experiments with 2 μM free calcium. Results marked *1* are with calcium-free solution during the test period, and results marked *3* are with 50 μM free calcium during the test period.

Two experiments are presented in Fig. 4. Squares (*1*) give results obtained for recovery in the absence of cytoplasmic calcium. Open and filled circles (*2*) give the results obtained for recovery in the presence of 2 μM free calcium for the two experiments. Triangles (*3*) are the results for recovery with 50 μM free calcium in the second experiment. As shown by the solid curves in Fig. 4, single exponential functions describe the data within the scatter of the observations. Recovery in the absence of free calcium takes place with a rate constant of 0.05 s^{-1} at 2 μM free calcium with rate constant of 0.2 s^{-1}, and at 50 μM free calcium with a rate constant of 0.9 s^{-1}.

The recovery from inactivation can be studied more conveniently by monitoring inward exchange current as described in Fig. 5. To do so, pipette solution B is used with 2 mM calcium and 150 mM sodium. The protocol is then to switch between a cytoplasmic solution with a chosen free calcium concentration without sodium and a cytoplasmic solution with 100 mM sodium and no calcium (see Fig. 5 *A*). Results in Fig. 5 *A* are for two different calcium concentrations (*1* is for 2 μM and *2* is for 50 μM). Different cytoplasmic calcium concentrations are first preapplied to induce the

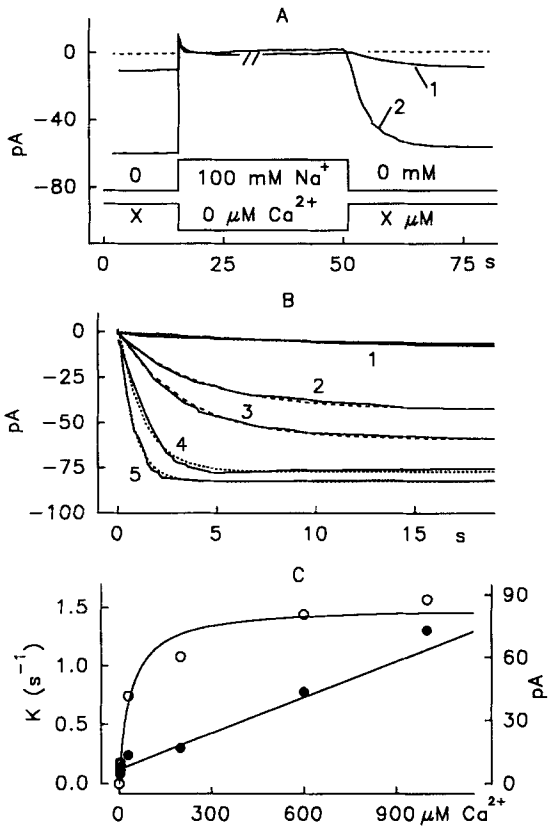

FIGURE 5. Recovery from sodium-dependent inactivation monitored with inward exchange current. The pipette solution contains 2 mM calcium and 150 mM sodium. (*A*) Protocol of solution switches used. A sodium-free, calcium-containing solution was switched to a 100 mM sodium, calcium-free solution, as indicated, followed by a return to the original calcium-containing solution. Results shown are with 2 and 50 μM free cytoplasmic calcium, marked *1* and *2*, respectively. (*B*) A series of inward current recovery curves with fitted exponentials given as dotted lines. Cytoplasmic calcium concentrations are 2 μM (record *1*), 4 μM (record *2*), 50 μM (record *3*), 600 μM (record *4*), and 1000 μM (record *5*). (*C*) The cytoplasmic calcium dependence of steady-state inward current (*open circles*, pA) and the recovery rate constants (*filled circles*, *k*). Current amplitudes and rate constants are fitted to a hyperbola (*solid curve*) and a straight line, respectively. Note that the recovery rate continues to increase in the range of hundreds of micromolar free calcium, while the fitted half-saturation of inward current occurs at 25 μM free calcium.

inward exchange current, whereby the inward current can be activated and turned off within solution switch times in the absence of cytoplasmic sodium (not shown; see Figs. 9 and 10 of Hilgemann et al., 1992). Upon application of sodium and removal of calcium a small outward current transient is seen. Upon removal of cytoplasmic sodium and reapplication of cytoplasmic calcium at the same concentration as before, the inward current turns on slowly. As shown in Fig. 5 *B* for five different calcium concentrations, the recovery curves are well fit by single exponentials (dotted lines).

The magnitudes of the inward exchange current and the rate constant of recovery both increase as the cytoplasmic calcium concentration is increased.

The rate constants of the recovery curves and the steady-state inward current are plotted in Fig. 5 *C* against the cytoplasmic calcium concentration. Note that the steady-state inward current (open circles) has relatively low apparent calcium affinity in this experiment. It is activated by 50% at 25 μM free calcium. Note, furthermore, that the rate of recovery from inactivation (filled circles) continues to increase over the range of hundreds of micromolar in this experiment. There is a clear dissociation between the calcium dependence of the inward current and the calcium dependence of the recovery from inactivation. Finally, note that the recovery rates appear to increase biphasically with increasing calcium concentration, first more markedly in the range of 10–40 μM free calcium, and then almost linearly over the range of hundreds of micromolar. For experiments both with inward and with outward currents, the rate of recovery from I_1 inactivation appeared to increase up to the highest free cytoplasmic calcium concentrations used (1 mM).

Outward Current Decay upon Removal of Cytoplasmic Calcium

Since two processes seem to be involved in the modulation of exchange current by cytoplasmic calcium (Fig. 2), the turn-off of outward exchange current upon removal of cytoplasmic calcium should reflect the simultaneous operation of both mechanisms. If one mechanism allows a faster transition to an inactive state, that mechanism will, of course, dominate the time course of current decay upon removing cytoplasmic calcium. Figs. 6 and 7 show two of the protocols used to test for the expected mechanistic multiplicity and to approximate the relative rates of the two processes.

The first protocol was to examine the time courses of current decay when the cytoplasmic calcium was decreased from a given high concentration to different low concentrations in the presence of 100 mM cytoplasmic sodium. Fig. 6 shows a typical experiment with results numbered in the order in which the experiment was performed. The time course of current decay was first monitored upon switching free calcium from 50 to 0 μM (curve *1*). 50 μM free calcium was then reapplied (not shown) and free calcium was subsequently reduced from 50 to 7 μM (curve *2*). Similarly, cytoplasmic calcium was decreased from 50 to 18 μM (curve *3*) and from 50 to 0 μM free calcium (curve *5*). Current record *4* is for a reduction of the free calcium concentration from 7 to 0 μM. Spikes of the outward exchange current were observed when cytoplasmic calcium concentration was decreased from 50 μM, and these spikes probably reflect the immediate disinhibition of the outward current by removal of the high cytoplasmic free calcium, because calcium and sodium compete directly for transport sites. The decay curves are all well fit by single exponentials, given in Fig. 6 as dotted lines. As plotted in the inset, the rate constant of current decay upon removing cytoplasmic calcium increases as calcium is decreased to lower concentrations. The rate approximately doubles between 7 μM (trace *2*) and 0 μM (traces *1* and *5*) free calcium (three similar observations, one experiment with no apparent effect). From analysis of >20 decay curves, it is reported that a clear separation of two components in the decay curves was never obtained; in the great majority of cases single-exponential fits were as good as in Fig. 6. As pointed out in connection with

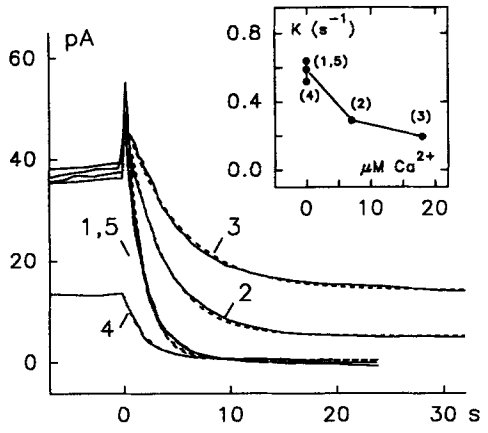

FIGURE 6. Time course of outward exchange current decay upon reducing cytoplasmic free calcium (pipette solution A, 5 mM calcium, and cytoplasmic 100 mM sodium). Results are numbered in the order in which the experiments were carried out. At the zero time in the figure, free calcium was reduced from 50 μM to 0, 7, 18, and 0 μM in the results marked *1*, *2*, *3*, and *5*, respectively. For the result marked *4*, cytoplasmic calcium was reduced from 7 to 0 μM. The dotted curves are single exponentials fitted to the decay curves. Note that all results are well fitted. The calcium dependence of rate constants obtained is plotted in the inset.

Fig. 3, the steady-state operation of I_2 inactivation has a calcium dependence in the submicromolar range. It is expected, therefore, that I_2 inactivation will contribute increasingly to the overall decay rate as calcium is decreased into the submicromolar range. Accordingly, decay rates at 0 μM free calcium should reflect the operation of both I_1 and I_2 inactivation, while the decay rates at high calcium concentrations should reflect only the I_1 process. The difference in decay rates at 0 μM calcium and 18 μM free calcium, ~0.4 s^{-1}, should roughly indicate the I_2 inactivation rate in the absence of calcium.

Fig. 7 presents the second protocol which attempted to separate the two processes. In this case, again using the outward exchange current, sodium-free, calcium-containing cytoplasmic solution was preapplied. Different concentrations of sodium

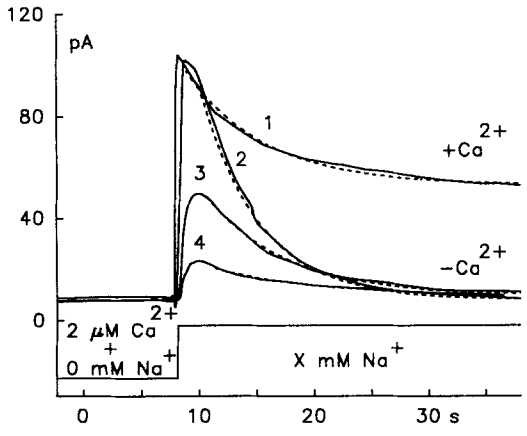

FIGURE 7. Outward exchange current decay curves at different cytoplasmic sodium concentrations. As indicated, sodium-free cytoplasmic solution was first applied with 2 μM free calcium. For the result marked *1*, 100 mM sodium was applied without changing the free calcium concentration. For the results marked *2–4*, calcium-free solution was applied with 100, 15, and 8 mM sodium, respectively. Dotted curves are single exponentials fitted to the results. Rate constants for results *1–4* are 0.15, 0.20, 0.15, and 0.10 s^{-1}, respectively.

were then applied and calcium was removed simultaneously. With low sodium concentrations, which induce only small amounts of I_1 inactivation, the rates of the decay obtained should reflect primarily the rate of I_2 inactivation. At high sodium concentrations, by contrast, the decay curves should reflect both the combined rates of the I_1 and I_2 processes. Curve *1* in Fig. 7 shows the current transient obtained upon applying 100 mM sodium without removing calcium. Curves *2–4* are with 100, 15, and 8 mM sodium, respectively. Note that curves *3* and *4* are rounded, where ~1 second was needed to reach peak current. This patch membrane rose up in the pipette ~40 μm. The results thus give one example in this article of records where a current time course with good certainly represents diffusion to the membrane. The true diffusion time course becomes apparent only when nonsaturating ion concentrations are applied.

As indicated by the dotted lines in Fig. 7, all of these results are also reasonably described by single exponentials. The rate constant for curve *1* with 100 mM sodium and 2 μM free calcium is 0.15 s^{-1}. For curve *2* with 100 mM sodium and zero calcium applied simultaneously, the rate constant is 0.20 s^{-1}. For curve *3* with 15 mM sodium and no calcium, the rate constant is reduced to 0.15 s^{-1}, and for the curve *4* with 8 mM sodium the rate constant is 0.10 s^{-1}. Evidently, the rate constant for inactivation by the I_2 process is ~0.1 s^{-1} in this patch. In any case, it cannot be more than 0.1 s^{-1}. Note that curves *3* and *4* cross over curve *2* with higher sodium during their decay. This reflects the smaller decay rates as sodium, and thereby I_1 inactivation, is decreased.

Implications of the Modulation for Steady-State Ion Dependencies of the Inward Exchange Current

We point out here implications of the modulation by calcium for steady-state ion dependencies of the exchange process, in particular for the inward exchange current. Since exchange function is modified by secondary calcium-dependent reactions, this must be accounted for in the calcium dependence of inward exchange current.

Results in Fig. 8 *A* show the usual calcium dependencies obtained for inward exchange current (pipette solution C) in the absence and presence of 20 mM sodium. In the absence of sodium (filled circles) the calcium dependence is simple and is well fitted by a rectangular hyperbola. In the presence of 20 mM cytoplasmic sodium (open circles), however, the calcium dependence curve shows a "foot" and has an S shape (three observations). The Hill slope coefficient here is 1.2. A logical explanation is that increasing calcium concentrations induce recovery from I_1 inactivation, and this is readily reproduced in simple simulations (see Fig. 14). Note that the inward current is reduced by cytoplasmic sodium, even at the highest cytoplasmic calcium concentrations.

After obtaining the data presented in Fig. 8 *A*, the patch was treated with 1 mg/ml chymotrypsin for 1 min to functionally remove the inactivation processes, and the protocols were repeated. The foot of the calcium concentration–current relation in the presence of sodium is entirely removed. Half-maximum concentrations (K_h) in the presence of sodium decreased from 5.7 to 3.4 μM after chymotrypsin. In the absence of cytoplasmic sodium, the I_2 modulation can be expected to play a role. However, the K_h decreased only slightly, from 3.4 μM before chymotrypsin to 2.9 μM

after chymotrypsin. Since calcium dependence of the I_2 modulation is in the submicromolar range (Fig. 3 *B*), a large effect would be expected only at very low calcium concentrations. Note that the maximum current is still reduced by sodium. This is accounted for in models of the exchange cycle, described in an accompanying article (Matsuoka and Hilgemann, 1992) by the assumption that one sodium ion can still bind to the calcium-loaded exchanger on the cytoplasmic side.

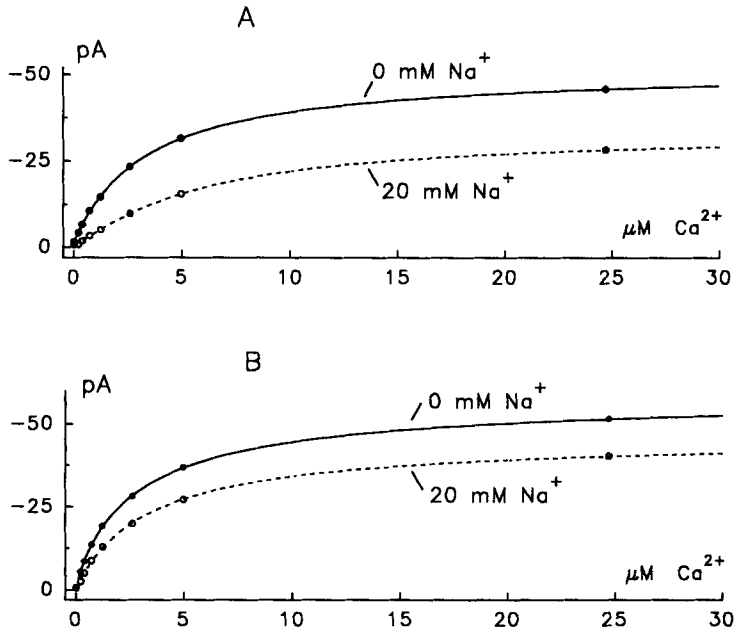

FIGURE 8. Effect of sodium-dependent inactivation on cytoplasmic calcium dependence of inward exchange current. Pipette solution C. (*A*) Before chymotrypsin treatment. (*B*) After application of 1 mg/ml chymotrypsin for 1 min. Note that the control relationship in the presence of sodium rises slowly in a low free calcium concentration range, and then more steeply from ~0.5 μM upward. This foot is entirely absent after chymotrypsin. See text for further details and explanations.

Possible Multiplicity of Inactive Exchanger States

In the study of channels, a delay or an S-shaped time dependence of activation with voltage steps is indicative of multiple transitions through inactive states to the active state(s). In our exchanger studies we sometimes observe delays in the onset of secondary activation by calcium, whereas we do not observe delays in the decline of outward exchange current upon removal of calcium or in the onset of inactivation upon application of cytoplasmic sodium. Small delays in the range of 100–300 ms may be determined entirely by solution switch kinetics and ion diffusion to the patch membrane. Particularly in patches that show low-affinity calcium regulation (i.e., with secondary modulation in the range of tens to hundreds of micromolar free calcium), however, we are confident that the longer delays obtained are not determined by solution switching or ion diffusion times. Fig. 9 shows a typical example.

The records in Fig. 9 are for activation of outward exchange current by cytoplasmic calcium in the presence of 100 mM cytoplasmic sodium with the usual solutions (pipette solution A). Upon switching to 50 μM free calcium from calcium-free solution (record *1*), the outward current rises with a distinct S shape. Upon switching back to calcium-free solution, the outward current first increases rapidly, as the direct inhibitory effect of high cytoplasmic calcium is removed, and then declines monotonically to baseline. The speed of the rapid increase of outward current presumably reflects the time course of the solution change. When 5 μM free calcium is preapplied (record *2*), the current rises with no delay upon application of the 50 μM free calcium. This phenomenon, when present, is completely reversible and is highly reproducible over the course of an experiment. To reproduce the wave form of record *1* by a product of asymptotic exponentials, six exponential functions must be multiplied (dotted curves). A similar S-shaped delay was also obtained upon activating the inward current by cytoplasmic calcium in patches from such myocyte batches

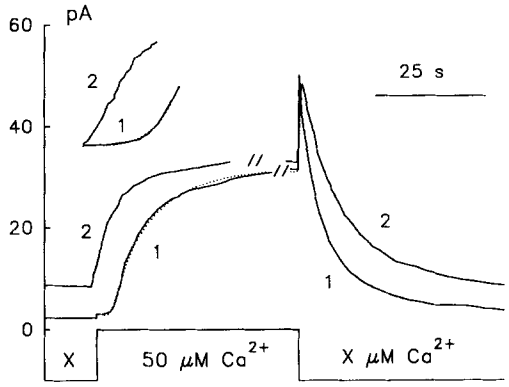

FIGURE 9. Time course of activation of outward exchange current by cytoplasmic calcium in a patch with low-affinity calcium modulation. For results marked *1*, a solution with 50 μM free calcium was applied from zero calcium as indicated. Note the delay in current activation and the fast current overshoot upon removal of cytoplasmic calcium. For results marked *2*, the solution switch is from 5 μM free cytoplasmic calcium to 50 μM and back. Note that the current onset is immediate and almost linear. The dotted curve is the fit of a product of six exponentials to the data. The inset shows the current onset at higher resolution.

(not shown). The delay in the activation of inward exchange current could be eliminated by chymotrypsin treatment.

For the analysis of exchange function the possible existence of multiple active exchanger states is of great concern, and the majority of our experiments give no clear evidence for this complication. We note, however, one complex pattern occasionally observed which can be interpreted in this way. When the exchanger is highly activated by MgATP and/or phosphatidylserine (Hilgemann and Collins, 1992), the outward current induced by 100 mM cytoplasmic sodium sometimes had a slowly activating phase over the course of ~1 min after sodium-dependent inactivation (data not shown for brevity). During this time, the apparent sodium dependency of outward current was found to shift from a half-maximum of ~18 mM to a half-maximum of ~30 mM.

ATP Accelerates Recovery from I_1 Inactivation

As mentioned in the Introduction, the effects of MgATP on exchange current are to some extent similar to those of cytoplasmic calcium (e.g., reduction of sodium-dependent inactivation). Fig. 10 presents results on the recovery of inward sodium-calcium exchange current from sodium-dependent inactivation. In this case, pipette solution B was used with 150 mM sodium and 2 mM calcium. The entire experiment was performed in the presence of 3 μM free cytoplasmic calcium. The solution switches are from 0 to 100 mM cytoplasmic sodium and back to 0 sodium. Dotted

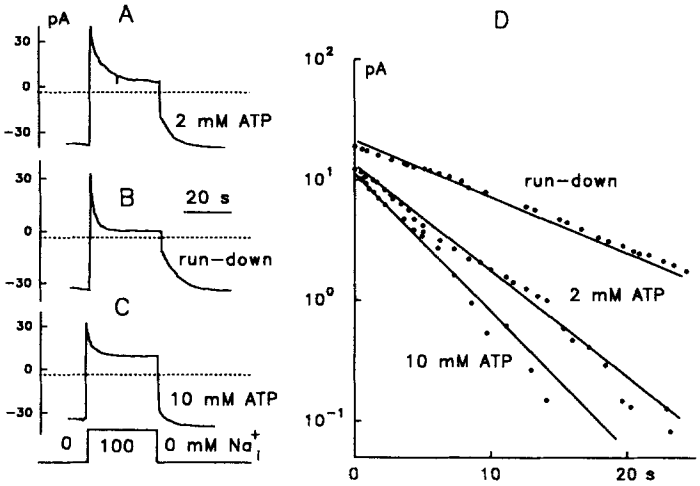

FIGURE 10. Analysis of MgATP effect on sodium-dependent inactivation kinetics. Results are with 2 mM calcium and 150 mM sodium in the pipette. Current transients were recorded for cytoplasmic solution switches from a solution containing sodium-free cytoplasmic solution with 3 μM free calcium to one with 100 mM sodium and 3 μM free calcium, and back to the original solution. Dotted lines give the current level in the absence of cytoplasmic calcium and sodium. Records were first obtained in the presence of 2 mM MgATP (*A*). ATP was then washed out and the current transients became more pronounced over 20 min (*B*). Finally, 10 mM ATP was applied and the current transients became much less pronounced (*C*). The slow recovery portions of the records upon switching back to sodium-free solution were fitted to exponentials and are plotted semi-logarithmically after subtracting an asymptote (*D*). The rate constants for run-down, 2 mM ATP, and 10 mM ATP are 0.09, 0.18, and 0.34 s^{-1}, respectively.

lines mark the current level for the sodium-free, calcium-free solution, which is assumed to be the zero exchange current level.

In this experiment, the patch was first superfused with 2 mM MgATP (Fig. 10 *A*), ATP was washed out, and the protocol was repeated several times during the next 15 min. After run-down of the ATP effect, inactivation of the outward current during application of sodium was substantially more pronounced and more rapid (Fig. 10 *B*). Correspondingly, the slow recovery phase of inward current constitutes a larger fraction of the total inward current. After the record in Fig. 10 *B* was obtained, 10 mM MgATP was superfused. The outward current is increased and the inactiva-

tion phase is substantially decreased. Correspondingly, the recovery phase of the inward current is relatively small. The steady-state inward current in the absence of sodium shows little change with MgATP.

The recovery phases of the three records were fit to single exponentials and the results are plotted in Fig. 10 *D* in semi-log fashion. The rate constant of the recovery after application of 10 mM ATP (0.34 s^{-1}) is about four times greater than after current run-down (0.09 s^{-1}), and the rate with 2 mM ATP (0.18 s^{-1}) is intermediate. Thus, MgATP accelerates recovery from sodium-dependent inactivation to an extent

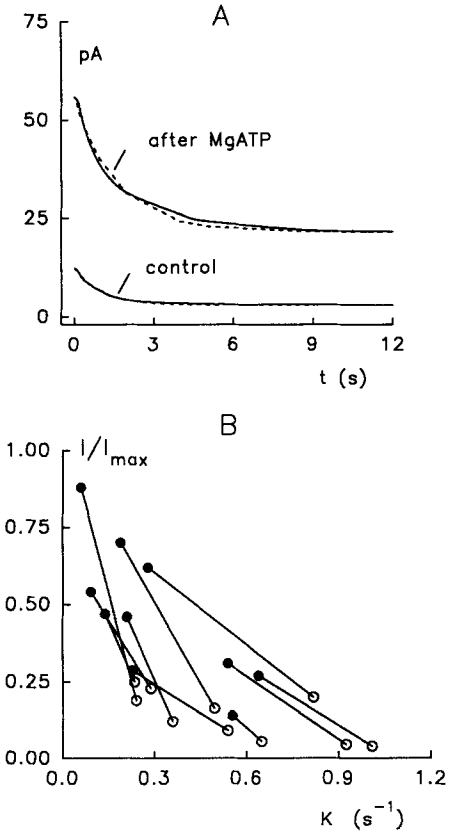

FIGURE 11. Effect of MgATP on outward exchange current transients during cytoplasmic application of 100 mM sodium. Pipette solution A. 2 μM cytoplasmic free calcium. 2, 4, or 6 mM MgATP. (*A*) Examples of outward current transients before and after application of 2 mM MgATP. Dotted curves are single exponentials fitted to the data. (*B*) Rate constants of inactivation and steady-state current magnitudes before (*open circles*) and after MgATP (*filled circles*) are connected by lines for eight experiments. Steady-state current magnitudes (I/I_{max}) are normalized to the current magnitude of each patch after ATP immediately upon application of sodium (I_{max}). In each patch, MgATP substantially increased the steady-state exchange current and decreased the rate constant of inactivation.

that could explain much of the increase of exchange current in the presence of cytoplasmic sodium.

ATP Slows Entrance into I_1 Inactivation

Fig. 11 presents the effect of MgATP on outward exchange current transients during application of 100 mM sodium in the presence of 2 μM free cytoplasmic calcium. As shown in the example experiment in Fig. 11 *A*, exchange transients before and after application of 2 mM MgATP were fitted to single exponentials (dotted lines). The

results are presented in Fig. 11 *B*, where steady-state current magnitudes are normalized in each experiment to the peak current obtained immediately upon application of sodium after MgATP (I_{max}). Results before and after MgATP are connected by lines in Fig. 11 *B*, where the "after ATP" current is greater in each experiment. The rate constant of the current transient was decreased in every case when MgATP had a substantial stimulatory effect. Accordingly, each point after ATP is located to the upper left of the point before ATP.

As with the effect of cytoplasmic calcium, there is evidently a dual effect of ATP on the sodium-dependent inactivation process (I_1 modulation). The rate of recovery from inactivation upon removal of sodium increases, and the current decay during application of sodium becomes slower. As with the effect of cytoplasmic calcium, the rate constant determined during application of sodium can be assumed to reflect a

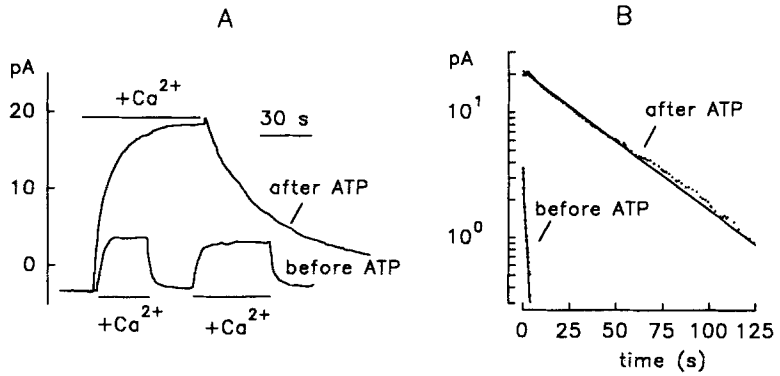

FIGURE 12. Effect of MgATP on kinetics of outward exchange current with changes of cytoplasmic calcium. Results are from a patch with a very large and maintained stimulatory effect of MgATP. (*A*) Application and removal of 2 μM free calcium in the presence of 100 mM cytoplasmic sodium. Note that the initial rate of rise of current upon application of calcium is almost unchanged by MgATP, while the decay rate upon removal of calcium is drastically slowed. (*B*) Decay of outward exchange current upon removal of cytoplasmic calcium before and after MgATP. An asymptote was subtracted and results are plotted semi-logarithmically.

sum of the forward and backward rate constants, and accordingly it must be concluded that the rate of inactivation is decreased by ATP while the rate of recovery from activation is increased.

ATP Slows Outward Current Decay on Removal of Cytoplasmic Calcium

Another perspective on the action of MgATP is gained from the kinetics of outward exchange current decay and recovery during removal and reapplication of cytoplasmic calcium. As shown in Fig. 12, a large stimulatory effect of MgATP can be accompanied by a drastic reduction in the rate of current decay upon removal of cytoplasmic calcium. In this patch, the outward current decayed by ~80% on application of sodium before MgATP, and the current decayed by only ~10% after MgATP. Fig. 12 *A* shows the outward exchange current responses to application and

removal of 2 μM free cytoplasmic calcium. Before application of MgATP, the current can be turned on and off to ~80% equilibration in just 6 s. After MgATP, the current is increased in the presence of calcium by a factor of ~4, and calcium must be applied for ~30 s to achieve 80% equilibration. Note that the initial rate of current change upon application of calcium is almost unchanged by MgATP. Fig. 12 *B* shows the current decay records in semi-log plot after subtraction of an asymptote. Both records are well fitted by a single exponential. Both the I_1 and I_2 modulation processes are expected to influence this time course.

Implications of the Modulation for Steady-State Ion Dependencies of the Outward Exchange Current

An important implication of sodium-dependent inactivation (I_1 modulation) for the ion dependence of outward exchange current is presented in Fig. 13. The results shown are the steady-state cytoplasmic sodium dependence of outward exchange

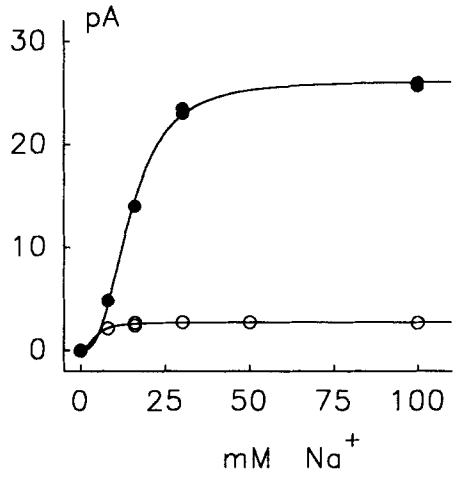

FIGURE 13. Effect of strong stimulatory effect of MgATP on cytoplasmic sodium dependence of outward exchange current. Open circles give the steady-state cytoplasmic sodium dependence of outward exchange current before and filled circles after application of 5 mM MgATP. The exchange current before ATP showed strong sodium-dependent inactivation and after ATP showed almost no sodium-dependent inactivation. Note that the half-maximum sodium concentration shifts strongly to the right after ATP.

current before (open circles) and after (filled circles) application of 5 mM MgATP. Before ATP, the fitted half-maximum sodium concentration is 5 mM. After ATP, the half-maximum concentration is 18 mM. Similar results have been obtained with the loss of inactivation by chymotrypsin (not shown). An explanation, readily verified in simple simulations, is that the sodium concentration dependence of the current is self-limiting in the presence of strong inactivation. As sodium is increased more current is activated, but simultaneously a greater fraction inactivates. We note that our explanations of the MgATP effect do *not* explain the increase of apparent extracellular sodium affinity observed in squid axon with application of MgATP (Blaustein, 1977). Equivalent data are not available for the cardiac exchanger.

DISCUSSION

The dynamic behaviors of cardiac sodium-calcium exchange current, revealed with the giant patch method, were largely unexpected from previous studies of the

sodium-calcium exchange process, and to our knowledge have no obvious precedent in measurements with other ion transporters. As sketched in the Results and described in the Appendix, we interpret these patterns quantitatively in terms of two independent modulation processes that can move the exchanger into completely inactive states. It is expected that these processes control the physiological function of the exchanger, similar to the voltage- and ligand-dependent gating of ion channels. In the following sections we discuss details of our interpretation, as well as weaknesses of the interpretation and possible contradictions on the basis of available data and the simulations presented in the Appendix.

Analysis and Interpretation of Dynamic Exchange Modulation

The central assumption of our analysis is that exchange current transients represent transitions between an active state and fully inactive exchanger states. The function of the active state would correspond essentially to that of the chymotrypsin-deregulated exchanger. In a first approximation, the two modulation processes would be independent reactions. In pursuing this analysis, our goal has been to account for the most possible significant observations with the fewest possible assumptions, and the majority of our observations are indeed well accounted for (see Appendix for documentation of explanatory range). Evidence for additional complications has arisen primarily under boundary conditions, as a delay in secondary activation by cytoplasmic calcium in membranes with low-affinity calcium regulation (Fig. 9). In addition to this complication, it appears significant that the measured dependencies of modulation kinetics on cytoplasmic calcium (middle graph in Fig. 3 *B*; Fig. 5 *C*) are complex. This could be indicative of regulation via more than one calcium binding site.

In spite of these and other possible complications (e.g., speculation about multiple stoichiometries with different electrogenicities [Mullins, 1991] or heterogeneity of enzyme conformations, as can occur with the band 3 anion transporter [Swanson, Keast, Jennings, and Pessin, 1988]), our analysis provides a simple conceptual framework to account for an otherwise very complex pattern of responses. Above all, the analysis establishes guideposts for further experimental and theoretical work on the molecular basis of dynamic exchange modulation and the control of physiological exchange function.

Of course, other types of experimentation and experimental approaches are needed to elucidate the physical basis of the modulation mechanisms, starting with the question of whether auxiliary proteins are involved. Up to now, only one experimental result suggests that a cofactor might dissociate under some conditions with a resulting loss of the modulation processes. In patches from mouse myocytes, the regulatory properties can be irreversibly lost during application of MgATP (Collins et al., 1992). Apart from this, effects of several interventions that might dissociate proteins were entirely reversible. Observations included the effects of strong alkalosis (Hilgemann et al., 1992), chaotropic ions, and large ionic strength changes (Hilgemann, D. W., unpublished observations). Importantly, when the cloned cardiac exchanger (Nicoll, Longoni, and Philipson, 1990) is expressed in *Xenopus* oocytes, the modulation processes coexpress with sodium-calcium exchange current activity (Matsuoka, S., D. A. Nicoll, R. F. Reilly, D. W. Hilgemann, and K. D.

Philipson, manuscript submitted for publication). Thus, the great majority of observations suggest that the modulation properties are intrinsic to the exchanger itself, and are mediated by a cytoplasmic exchanger domain or domains.

In our simulations, we assume that I_1 and I_2 modulations are controlled by the same calcium regulatory site, but we have no reason to assume that only one site is involved. Only the identification of one or more regulatory calcium binding sites within the cytoplasmic loop of the exchanger or the identification of exchanger-associated calcium binding proteins will resolve the open issues. Up to now, our attempts to modify the function of native and cloned cardiac exchangers by exogenously introducing calcium binding proteins, namely calmodulin and annexin IV, have been completely negative (Matsuoka, S. and D. W. Hilgemann, unpublished observations).

As an alternative to the existence of regulatory binding sites, secondary modulation by cytoplasmic calcium might involve calcium binding to transport sites of the exchanger. Inactive conformations of the exchanger might exist that could still bind calcium at transport sites, and occupation by calcium would favor transition back to an active state. Since sodium and calcium functionally displace one another in the transport function (Reeves and Sutko, 1983; Miura and Kimura, 1989; Matsuoka and Hilgemann, 1992), it would be surprising if competition between sodium and calcium is not operative in the secondary activation process (Fig. 1).

One further plausible mechanism of secondary modulatory reactions is that the exchanger might form functionally interdependent dimers or heterooligomers. The existence of oligomeric units is well established for the anion exchanger, although functional implications are not well established (e.g., Boodhoo and Reithmeier, 1984). For the GLUT1 glucose transporter, oligomerization has recently been suggested to be important in determining transport kinetics (Hebert, D. N., and A. Carruthers, manuscript submitted for publication). The sarcolemmal calcium pump can oligomerize, and the oligomerized enzyme is established to be a highly activated enzyme form (Vorherr, Kessler, Hofmann, and Carafoli, 1991). The calcium pump dimerization evidently can take place via the calmodulin binding region (Vorherr et al., 1991), and homologous regions exist in the cardiac sodium-calcium exchanger (Nicoll et al., 1990).

Modulation of Sodium-dependent (I_1) Inactivation by Cytoplasmic Calcium and MgATP

Both calcium and MgATP decrease I_1 inactivation by accelerating the recovery from inactivation and, according to our analysis, by decreasing the rate of entrance into inactivation. Presumably, both the binding of calcium and the action of some second messenger in response to MgATP can stabilize the active state in an allosteric fashion, thereby affecting both the inactivation and recovery rates. It remains entirely uncertain what, if any, final link there might be between the action of cytoplasmic calcium and MgATP.

I_2 Modulation

Our analysis of I_2 modulation is limited because the transition from the I_2-inactive state to the active state is usually as fast (100–200 ms), or nearly as fast, as our

solution switch time. Up to now, we see no evidence that the I_2 modulation depends on specific configurations of transport sites per se, or on ion binding to transport sites. Much more work is needed to test the numerous possibilities that arise from these considerations. It should be readily possible to study the I_2 modulation with optimized solution switching techniques in patches that do not rise up in the pipette tip. Finally, it is important to point out that I_2 modulation is likely to be the major determinant of the secondary activation of outward exchange current by cytoplasmic calcium in whole myocyte studies (e.g., Kimura et al., 1987). That is because under common conditions of myocyte experiments (high cytoplasmic MgATP concentrations, less-than-saturating cytoplasmic sodium concentrations, and less-than-saturating extracellular calcium concentrations) the role of I_1 modulation (sodium-dependent inactivation; Hilgemann et al., 1992) is likely to be minimized. While the calcium dependence of I_2 modulation in giant membrane patches is usually in the range of hundreds of nanomolar free calcium, the activation of outward current in intact myocytes by free cytoplasmic calcium takes place in a several-fold lower concentration range. An apparent K_m of 47 ± 16 nM is given by Noda et al. (1988), and an apparent K_m of 22 nM is given by Miura and Kimura (1989). The reasons for these discrepancies remain to be clarified.

Relationships of I_1 and I_2 Modulation

In the Appendix, the two modulation processes are treated as independent reactions. Previously, a set of simulations were presented in which the two processes were treated interactively (Hilgemann et al., 1991). At that time, data on the modulation of sodium-dependent inactivation by cytoplasmic calcium were not available, and the specific scheme used failed with the more detailed observations (Figs. 3–6). Further experimentation and analysis will be needed to test whether or not the two modulation reactions are indeed interactive. Given evidence that both calcium and MgATP act on both processes, it would be surprising if an interactive relationship did not exist.

Physiological Significance of Modulation Mechanisms

It is striking that the exchanger is modulated secondarily by both ions that it transports. A role of I_2 modulation in control of exchange function in calcium homeostasis can be easily envisioned, while the function of I_1 modulation is less apparent. I_2 modulation should result in a slow (multi-second) turn-off of calcium extrusion as calcium falls into the submicromolar range. Accordingly, it may be a major determinant of the resting free calcium in cardiac cells (for further discussion see Hilgemann, 1990*b*). With respect to I_1 modulation, it must first be determined whether this process is operational in an intact cardiac cell. If so, the question emerges as to why the exchange system should be turned off secondarily in response to a rise of cytoplasmic sodium. A teleological argument may be derived from the thermodynamic consideration that the exchanger cannot establish a low resting free calcium concentration when cytoplasmic sodium is high. The exchanger is then a potential calcium "overload" mechanism, and the sodium-dependent inactivation process might serve to avoid the overload. It is an attractive, but still entirely

speculative, possibility that I_1 modulation via MgATP and negatively charged phospholipids is linked to regulatory systems of the cardiac cell.

Finally, we point out that the I_1 and I_2 modulation reactions under different circumstances can be expected to support either a positive feedback with respect to calcium influx or a negative feedback with respect to calcium extrusion. Accordingly, the modulation mechanisms are candidates for a role in phasic changes of cytoplasmic calcium such as calcium oscillations.

APPENDIX

We describe here how the assumed existence of two independent inactivation processes can account for most of the dynamic modulatory properties of exchange current described in this article. As described in the preceding article (Hilgemann et al., 1992), the function of sodium-dependent inactivation (I_1 inactivation) at a constant free cytoplasmic calcium concentration can be described as a linear, monomolecular reaction, where the transition to the inactive state (α_1) is directly proportional to the fraction of total exchanger population fully loaded with sodium on the cytoplasmic side (F_{E13Na}) and the recovery from inactivation is assumed to be a simple, time-dependent reaction (β_1). To describe results presented in this article, we must further assume that these reactions are influenced by calcium binding to a neighboring regulatory site. For simplicity, this is assumed to be an instantaneous binding,

$$F_{Caact} = Ca_i/(Ca_i + K_{Caact}) \quad (1)$$

where F_{Caact} is the fraction of exchangers with calcium bound at the regulatory site, Ca_i is the free cytoplasmic calcium concentration, and K_{Caact} is the dissociation constant for calcium from the regulatory site. Under the assumption that calcium binding to the regulatory site stabilizes the active state of the I_1 modulation reaction (A_1), we expect that the forward and reverse reactions may be slowed and accelerated by roughly equal factors when calcium is bound (Scheme 1).

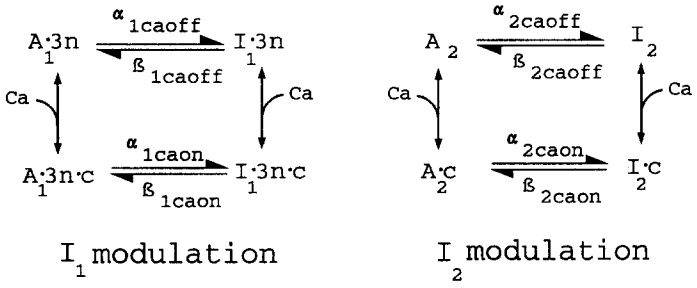

Accordingly, the inactivation rate in the presence of bound regulatory calcium (α_{1Caon}) is substantially lower than in the absence of bound regulatory calcium (α_{1Caoff}), and the rate of recovery from inactivation in the presence of bound regulatory calcium (β_{1Caon}) is substantially higher than in the absence of regulatory calcium (β_{1Caoff}). Now,

$$\alpha_1 = F_{E13Na} \times [F_{Caact} \times \alpha_{1Caon} + (1 - F_{Caact}) \times \alpha_{1Caoff}] \quad (2)$$

and

$$\beta_1 = F_{Caact} \times \beta_{1Caon} + (1 - F_{Caact}) \times \beta_{1Caoff} \quad (3)$$

For the purposes of this Appendix, the I_2 inactivation can be treated identically except that it has no dependence on the transport configuration of the exchanger. Calcium binding to the same regulatory site is assumed to modify this reaction:

$$\alpha_2 = F_{Caact} \times \alpha_{2Caon} + (1 - F_{Caact}) \times \alpha_{2Caoff} \tag{4}$$

and

$$\beta_2 = F_{Caact} \times \beta_{2Caon} + (1 - F_{Caact}) \times \beta_{2Caoff} \tag{5}$$

These equations can be used with any of the exchange cycle models described previously. We used the E2 model described in the following article (Matsuoka and Hilgemann, 1992), although for most of the goals of this Appendix a complete exchange model is not required. Abbreviated equations can be used as follows, since extracellular ion concentrations and membrane potential are not changed. First, the E2 description of competitive–noncompetitive interactions of cytoplasmic sodium and calcium is needed. In the E2 model, F_{ci} and F_{3ni} give the fractions of exchanger with cytoplasmic-oriented binding sites, which have bound and occluded one calcium ion and three sodium ions, respectively:

$$F_{ci} = (C_i/K_{ci})/D_i \tag{6}$$

$$F_{3ni} = [N_i^3/(K_{1ni} \times K_{2ni} \times K_{3ni})]/D_i \tag{7}$$

with

$$D_i = (C_i/K_{ci}) \times (1 + 1 + N_i/K_{cni}) + 1 + N_i/K_{1ni} + N_{i2}/(K_{1ni} \times K_{2ni}) + N_i^3/(K_{1ni} \times K_{2ni} \times K_{3ni}) \times (1 + 1) \tag{8}$$

where K_{ci} is a dissociation constant for calcium from the binding site and K_{1ni}, K_{2ni}, and K_{3ni} are dissociation constants for the first, second, and third sodium ion from binding sites. The 1 + 1 in the denominator arises from the assumption that equilibrium constants of the calcium occlusion reaction and of the three sodium occlusion reaction are 1. For the conditions of saturated transport sites on the extracellular side, it is assumed that one-half of exchangers with extracellularly oriented binding sites are available to transport ions to the cytoplasmic side. Accordingly, F_{E1Ca} and F_{E13Na} give the fractions of the total exchanger population that have bound and occluded one cytoplasmic calcium ion and three cytoplasmic sodium ions, respectively:

$$F_{E13Na} = F_{3ni}/[1 + (F_{3ni} + F_{ci}) \times 2] \tag{9}$$

$$F_{E1Ca} = F_{ci}/[1 + (F_{3ni} + F_{ci}) \times 2] \tag{10}$$

Finally, the outward (I_{out}) and inward (I_{in}) exchange currents can be calculated as

$$I_{out} = F_{E13Na} \times A_1 \times A_2 \tag{11}$$

$$I_{in} = F_{E1Ca} \times A_1 \times A_2 \tag{12}$$

Since the inactivation reactions are linear and independent, trivial explicit solutions are given for the A_1 and A_2 fractions at time t from their magnitudes (A_{1t0} and A_{2t0}) at zero time (t_0) and their steady-state magnitudes ($A_{1\infty}$ and $A_{2\infty}$):

$$A_1 = (A_{1\infty} - A_{1t0}) \times (1 - e^{-t \times (\alpha 1 + \beta 1)}) + A_{1t0} \tag{13}$$

$$A_2 = (A_{2\infty} - A_{2t0}) \times (1 - e^{-t \times (\alpha 2 + \beta 2)}) + A_{2t0} \tag{14}$$

where

$$A_{1\infty} = \beta_1/(\alpha_1 + \beta_1) \text{ and } A_{2\infty} = \beta_2/(\alpha_2 + \beta_2) \quad (15)$$

As described in the Results and elsewhere (Collins et al., 1992), the kinetics and particularly the apparent calcium dependencies of the inactivation reactions were rather variable from cell batch to batch. Accordingly, the results described have not been fitted simultaneously to the model equations. In Figs. 14–16, the predicted exchange current behaviors are presented for one set of parameters, generating results in roughly the mid-range of kinetics and calcium dependencies observed experimentally. The parameters used were: $K_{1ni} = 126$ mM, $K_{2ni} = K_{3ni} = 11$ mM, $K_{ci} = 18$ μM, $K_{Cact} = 0.04$ mM, $\alpha_{1Caoff} = 0.66$ s^{-1}, $\alpha_{1Caon} = 0.03$ s^{-1}, $\beta_{1Caoff} = 0.015$, $\beta_{1Caon} = 1$ s^{-1}, $\alpha_{2Caoff} = 0.25$ s^{-1}, $\alpha_{2Caon} = 0.00005$ s^{-1}, $\beta_{2Caoff} = 0.00025$ s^{-1}, and $\beta_{2Caon} = 50$ s^{-1}. The turnover rates given are consistent among figures in this Appendix.

Fig. 14 shows the simulated cytoplasmic calcium dependence of the steady-state outward and inward currents in panels *A* and *B*, respectively, at two cytoplasmic sodium concentrations. Analogous to Fig. 1, Fig. 14 *A* shows the simulated cytoplasmic calcium dependence of outward

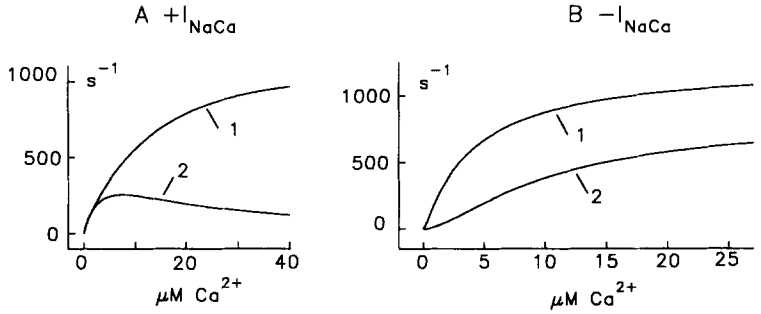

FIGURE 14. Simulated dynamic modulation properties of cardiac sodium-calcium exchange. See text for details. (*A*) Simulation 1 shows the cytoplasmic calcium dependence of outward exchange current with 90 mM sodium and simulation 2 with 18 mM sodium. Note the shift of the apparent affinity for cytoplasmic calcium. (*B*) Simulation 1 shows the cytoplasmic calcium dependence of inward exchange current without cytoplasmic sodium and simulation 2 with cytoplasmic sodium (20 mM). Note the development of a foot in the calcium–current relation.

current with 90 mM cytoplasmic sodium in simulation 1 and 18 mM sodium in simulation 2. At lower cytoplasmic sodium, less cytoplasmic calcium is needed to overcome I_1 inactivation, and secondary activation of outward current is shifted to lower calcium concentration. Note that the steady-state sodium dependence of outward current is completely saturated at 18 mM in the simulation in the low free cytoplasmic calcium range. That this can be the case experimentally, when inactivation is strong, was demonstrated in Fig. 13. Analogous to Fig. 8, the cytoplasmic calcium dependence of inward exchange current (Fig. 14 *B*) is monotonic, or nearly so, in the absence of cytoplasmic sodium (simulation 1) but develops a foot in the presence of 20 mM cytoplasmic sodium (simulation 2). At high calcium concentrations, the decrease of inward current with 20 mM cytoplasmic sodium is due to the binding of sodium to the calcium-occupied exchanger. The sodium-dependent inactivation itself can be entirely overcome by high cytoplasmic calcium.

Fig. 15 *A* gives the peak and steady-state dependencies of outward exchange current on cytoplasmic free calcium (pCa) for step increases of cytoplasmic sodium from 0 to 100 mM, as shown in panel *B*. The calcium dependence of the peak current is half-maximal at ~0.3 μM

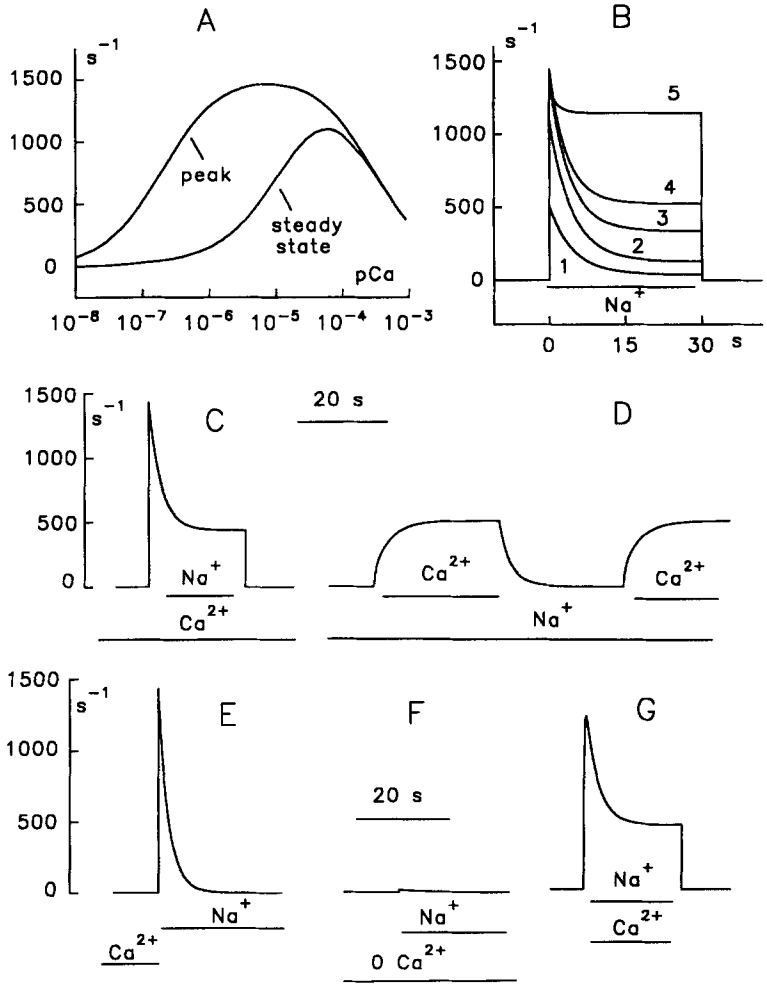

FIGURE 15. Simulated dynamic modulation properties of cardiac sodium-calcium exchange. See text for details. (*A*) Simulated cytoplasmic calcium dependence of peak and steady-state outward exchange current for application of 100 mM cytoplasmic sodium. (*B*) Simulated outward exchange current transients for application of 100 mM cytoplasmic sodium in the presence of 0.1, 0.5, 2, 4, and 50 μM free cytoplasmic calcium, respectively. (*C*) Simulated outward exchange current transient for application of 100 mM sodium, entirely in the presence of 3 μM free cytoplasmic calcium. (*D*) Simulated outward exchange current transient for a step increase of cytoplasmic free calcium from 0 to 3 μM, back to 0 μM, and again back to 3 μM, entirely in the presence of 100 mM cytoplasmic sodium. (*E*) Simulated outward exchange current transient for a solution switch from one with 3 μM free calcium and no sodium to one with no calcium and 100 mM sodium. (*F*) Simulated outward exchange current transient (or lack thereof) for a solution switch from one without calcium or sodium to one without calcium but with 100 mM sodium. (*G*) Simulated outward exchange current transient for a solution switch from one without calcium or sodium to one with 3 μM free calcium and 100 mM sodium. The corresponding experimental results for *A* and *B* are from Fig. 3. The corresponding experimental results for *C–G* are from Fig. 2.

and is determined by the equilibrium of the I_2 inactivation. The calcium dependence of the steady-state current, which is shifted by ~1 log unit to higher free calcium concentrations, is determined mainly by the equilibrium of I_1 inactivation. The decline of current at high calcium concentrations is determined by the antagonism of calcium for sodium at the binding site. These results are equivalent to Fig. 3 *B* (upper graph). They reproduce well similar experi-

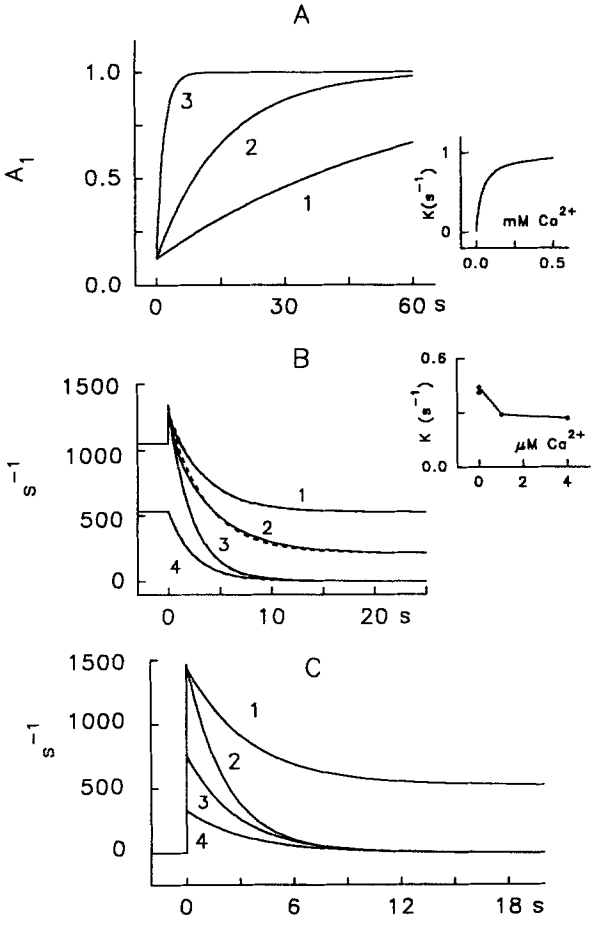

FIGURE 16. Simulated dynamic modulation properties of cardiac sodium-calcium exchange. See text for details. (*A*) Recovery of the I_1 modulation process from inactivation. The condition before time zero was a cytoplasmic solution with 100 mM sodium and 0.5 μM free calcium. At zero time, sodium was decreased to zero and a fraction of A_1 is plotted against time (s) with 0, 2, and 50 μM free calcium, respectively, in curves *1*, *2*, and *3*. The inset shows the dependence of the recovery rate constant on cytoplasmic free calcium. (*B*) Simulated exchange current transients for reduction of cytoplasmic free calcium concentration from 100 μM to 4, 1, and 0 μM, respectively, in curves *1*, *2*, and *3*. Curve *4* is for a reduction of cytoplasmic free calcium from 4 to 0 μM. Results are entirely in the presence of 100 mM cytoplasmic sodium. The inset gives the rate constants of exponentials (*dotted curves*) fitted to the decay curves. (*C*) Simulated outward exchange current transients starting from a cytoplasmic solution with 3 μM free calcium and no sodium. Curve *1* is for application of 100 mM sodium in the presence of 3 μM free calcium. Curve *2* is for application of 100 mM sodium with zero cytoplasmic calcium. Curves *3* and *4* are for application of 20 and 12 mM sodium, respectively, without cytoplasmic calcium. The corresponding experimental results for *A* are Figs. 4 and 5. The corresponding experimental results for *B* and *C* are Figs. 6 and 7, respectively.

ments in which the experimental protocols were extended over the full 5 pCa units given here (panel *C* of Fig. 2 in Hilgemann, 1990*a*). Fig. 15 *B* shows the simulated current transients for these protocols, equivalent to the results of Fig. 3. Curves *1–5* are for 0.1, 0.5, 2, 4, and 50 μM free calcium, respectively. The simulations are qualitatively equivalent to experimental results with respect to both the ratios of peak-to-steady-state current and the changes of kinetics as

calcium is increased. The acceleration of current decay between 4 and 50 μM free calcium is, however, less than that described in Fig. 3.

Fig. 15, *C–G* show the simulated responses to step changes of both sodium and calcium, equivalent to the results of Fig. 2. To simulate the appropriate ratio of peak-to-steady-state current for this particular experiment with the chosen simulation parameters, the simulations were carried out with 3 μM free cytoplasmic calcium instead of the 2 μM used experimentally. Fig. 15 *C* is the current transient for application of 100 mM sodium in the presence of 3 μM free calcium. Fig. 15 *D* shows the results for increasing and decreasing cytoplasmic calcium in the presence of sodium. Fig. 15 *E* shows the result of application of 100 mM sodium with simultaneous removal of the preapplied 3 μM free cytoplasmic calcium. Fig. 15 *F* shows the very small current transient expected for application of 100 mM sodium in the absence of calcium. Fig. 15 *G* shows the result for application of both sodium and calcium after preequilibration without calcium. The results are an accurate reproduction of experimental results in all respects, except for the cytoplasmic calcium dependence of outward current, which is variable from experiment to experiment. The calcium dependence of outward current in this simulation was in the high range of apparent affinities obtained experimentally.

Fig. 16 *A* shows the recovery from sodium-dependent inactivation at different cytoplasmic calcium concentrations, as described in Fig. 4. Fractions of A_1 are plotted against recovery time. Curve *1* gives recovery of I_1 inactivation at 0 mM cytoplasmic calcium, curve *2* is at 2 μM free calcium, and curve *3* is at 50 μM free calcium. The inset in *A* shows the complete calcium dependence of the rate constant of the I_1 process ($\alpha_1 + \beta_1$). Note that the simulated relationship saturates smoothly, and therefore the calcium dependence reflects quite accurately the assumed affinity of the regulatory binding site (K_d = 40 μM). This does not reproduce the results on inward current, presented in Fig. 5, where the rate constant of recovery continues to increase into the range of hundreds of micromolar.

Fig. 16 *B* shows the reproduction of the results from Fig. 6, where cytoplasmic calcium is reduced to different concentrations from a high concentration (100 μM) in the presence of 100 mM sodium. Curve *1* is for 4 μM, curve *2* is for 1 μM, and curve *3* is for 0 μM free calcium. Curve *4* is for calcium reduction from 4 to 0 μM free calcium. Single exponential fits to the simulated curves are plotted with the simulated results as dotted lines. The inset of Fig. 16 *B* shows the rate constants of the exponential fits to the different simulated results. Again, there is some quantitative discrepancy in the experimental results, consistent with the observed variability of experimentally measured rates, but the qualitative reproduction of experimental results is accurate.

Fig. 16 *C* shows simulated results equivalent to the protocol of Fig. 7. Curve *1* is the current transient for application of 100 mM sodium in the presence of 3 μM free cytoplasmic calcium. For curves *2–4*, calcium was removed together with application of 100, 20, and 12 mM sodium, respectively. Curves *3* and *4* cross over curve *2*, as is the case for the experimental results. Here as well, the kinetics of simulated results are not quantitatively correct, but the qualitative reproduction of data is entirely correct.

We thank Henry Liao and David P. Cash for technical assistance. Calmodulin and annexin IV were generous gifts of Drs. L. G. Tansey, J. T. Stull, and S. R. Sprang at this institution. We thank Dr. Shmuel Muallem for discussions and criticisms of an earlier version of this manuscript.

This work was supported by NIH grant R29 HL-45240, an Established Investigatorship, and a Grant-in-Aid of the American Heart Association to D. W. Hilgemann, and by a grant from the Japan Heart Foundation to S. Matsuoka.

Original version received 29 July 1992 and accepted version received 25 September 1992.

REFERENCES

Blaustein, M. P. 1977. Effects of internal and external cations and of ATP on sodium-calcium and calcium-calcium exchange in squid axons. *Biophysical Journal.* 20:79–110.

Boodhoo, A., and A. F. Reithmeier. 1984. Characterization of matrix-bound Band 3, the anion transport protein from human erythrocyte membranes. *Journal of Biological Chemistry.* 259:785–790.

Collins, A., A. V. Somlyo, and D. W. Hilgemann. 1992. The giant cardiac membrane patch method: stimulation of outward Na^+-Ca^{2+} exchange current by MgATP. *Journal of Physiology.* 454:27–57.

DiPolo, R. 1974. Effect of ATP on the calcium efflux in dialyzed squid giant axons. *Journal of General Physiology.* 64:503–517.

DiPolo, R. 1976. The influence of nucleotides on calcium fluxes. *Federation Proceedings.* 35:2579–2582.

DiPolo, R. 1979. Calcium influx in internally dialyzed squid giant axons. *Journal of General Physiology.* 73:91–113.

DiPolo, R., and L. Beaugé. 1987. Characterization of the reverse Na/Ca exchange in squid axons and its modulation by Ca_i and ATP. Ca_i-dependent Na_i/Ca_o and Na_i/Na_o exchange modes. *Journal of General Physiology.* 90:505–525.

DiPolo, R., and L. Beaugé. 1991. Regulation of Na-Ca exchange: an overview. *Annals of the New York Academy of Sciences.* 639:100–111.

Hilgemann, D. W. 1990*a*. Regulation and deregulation of cardiac Na^+-Ca^{2+} exchange in giant excised sarcolemmal membrane patches. *Nature.* 344:242–245.

Hilgemann, D. W. 1990*b*. 'Best estimates' of physiological Na/Ca exchange function: calcium conservation and the cardiac electrical cycle. *In* Cardiac Electrophysiology from Cell to Bedside. D. P. Zipes and J. Jalife, editors. W. B. Saunders Co, Philadelphia. 51–61.

Hilgemann, D. W., and A. Collins. 1992. Mechanism of cardiac Na^+-Ca^{2+} exchange current stimulation by MgATP: possible involvement of aminophospholipid translocase. *Journal of Physiology.* 454:59–82.

Hilgemann, D. W., A. Collins, D. P. Cash, and G. A. Nagel. 1991. Cardiac Na^+-Ca^{2+} exchange system in giant membrane patches. *Annals of the New York Academy of Sciences.* 639:126–139.

Hilgemann, D. W., S. Matsuoka, G. A. Nagel, and A. Collins. 1992. Steady-state and dynamic properties of cardiac sodium-calcium exchange. Sodium-dependent inactivation. *Journal of General Physiology.* 100:905–932.

Kimura, J., S. Miyamae, and A. Noma. 1987. Identification of sodium-calcium exchange current in single ventricular cells of guinea-pig. *Journal of Physiology.* 384:199–222.

Matsuoka, S., and D. W. Hilgemann. 1992. Steady-state and dynamic properties of cardiac sodium-calcium exchange. Ion and voltage dependencies of the transport cycle. *Journal of General Physiology.* 100:963–1001.

Miura, Y., and J. Kimura. 1989. Sodium-calcium exchange current. Dependence on internal Ca and Na and competitive binding of external Na and Ca. *Journal of General Physiology.* 93:1129–1145.

Mullins, L. J. 1991. Is stoichiometry constant in Na-Ca exchange? *Annals of the New York Academy of Sciences.* 639:96–98.

Nicoll, D. A., S. Longoni, and K. D. Philipson. 1990. Molecular cloning and functional expression of the cardiac sarcolemmal Na^+-Ca^{2+} exchanger. *Science.* 250:562–565.

Noda, M., R. N. Shepherd, and D. C. Gadsby. 1988. Activation by $[Ca]_i$ and block by 3′4′-dichlorobenzamil of outward Na/Ca exchange current in guinea-pig ventricular myocytes. *Biophysical Journal.* 53:342*a*. (Abstr.)

Rasgado-Flores, H. E., E. M. Santiago, and M. P. Blaustein. 1988. Kinetics and stoichiometry of coupled Na efflux and Ca influx (Na/Ca exchange) in barnacle muscle cells. *Journal of General Physiology*. 93:1219–1241.

Reeves, J. P., and J. L. Sutko. 1983. Competitive interactions of sodium and calcium with the sodium-calcium exchange system of cardiac sarcolemmal vesicles. *Journal of Biological Chemistry*. 258:3178–3182.

Requena, J. 1978. Calcium efflux from squid axons under constant sodium electrochemical gradient. *Journal of General Physiology*. 72:443–470.

Swanson, M. L., R. K. Keast, M. L. Jennings, and J. E. Pessin. 1988. Heterogeneity in the human erythrocyte Band 3 anion-transporter revealed by Triton X-114 phase partitioning. *Biochemical Journal*. 255:229–234.

Vorherr, T., T. Kessler, F. Hofmann, and E. Carafoli. 1991. The calmodulin-binding domain mediates the self-association of the plasmic membrane Ca^{2+} pump. *Journal of Biological Chemistry*. 266:22–27.